SCIENTIFIC REPORTS

OPEN

Electric Bias Induced Degradation in Organic-Inorganic Hybrid Perovskite Light-Emitting Diodes

Received: 7 June 2018
Accepted: 8 October 2018
Published online: 25 October 2018

Bing Xu[1,3], Weigao Wang[1], Xiaoli Zhang[1], Haochen Liu[1], Yuniu Zhang[1], Guanding Mei[1], Shuming Chen[1], Kai Wang[1,3], Liduo Wang[2] & Xiao Wei Sun[1,3]

For organic-inorganic perovskite to be considered as the most promising materials for light emitting diodes and solar cell applications, the active materials must be proven to be stable under various conditions, such as ambient environment, heat and electrical bias. Understanding the degradation process in organic-inorganic perovskite light emitting diodes (PeLEDs) is important to improve the stability and the performance of the device. We revealed that electrical bias can greatly influence the luminance and external quantum efficiency of PeLEDs. It was found that device performance could be improved under low voltage bias with short operation time, and decreased with continuous operation. The degradation of perovskite film under high electrical bias leads to the decrease of device performance. Variations in the absorption, morphology and element distribution of perovskite films under different electrical bias revealed that organic-inorganic perovskites are unstable at high electrical bias. We bring new insights in the PeLEDs which are crucial for improving the stability.

Organic-inorganic halide perovskite materials, methylammonium lead halide ($MAPbX_3$, X = Cl, Br, I) and formamidinium lead halide ($FAPbX_3$, X = Cl, Br, I), have attracted much attention for photovoltaic recently, due to high absorption coefficients, long charge carrier diffusion lengths and solution processability[1–5]. In less than five years, the power conversion efficiency of organic-inorganic perovskite (OIP) solar cell increased from 3.8% to 22%[6]. Being excellent light conversion materials, perovskites are also being considered as good light emitting materials, which have tunable band gaps, high color purity, benefit from facile solution processing, and low material cost[7–10]. Researchers made great efforts to improve the photoluminescence quantum yield and the device performance by compositional engineering, processing techniques, and interfacial engineering. The perovskite LEDs (PeLEDs) based on solution-processed method were first demonstrated by Tan *et al.* in 2014, which achieved a luminance of 364 cd m^{-2} and an external quantum efficiency (EQE) of 0.1%[11]. Recently, an EQE of 8.5% was reported for methylammonium lead bromide ($MAPbBr_3$)-based green LEDs[12] and 3.5% for methylammonium lead iodide ($MAPbI_3$)-based near-infrared LEDs[13], which are the highest EQEs reported so far for PeLEDs composed of pure $MAPbBr_3$ and $MAPbI_3$ films, respectively. More recently, an EQE of 8.8% was achieved for near-infrared LEDs using layered $PEA_2(CH_3NH_3)_{n-1}Pb_nI_{3n+1}$ (PEA = $C_8H_9NH_3$, phenylethylammonium) perovskite films[14] and an EQE of 11.7% was achieved by introducing excess large group ammonium halides in the precursor[15]. Despite these high efficiencies, the stability of the device under electric bias has not been well studied.

A well-known weakness of OIP is that they are moisture-sensitive and can degrade to PbX_2 after exposure to air. Besides material degradation, perovskite solar cell device also suffered significantly from electrical bias in different condition[16–21]. Tomas *et al.* found out that the application of an electric field in inert conditions lead to reversible degradation of perovskite thin film, but in presence of moisture lead to irreversible degradation[16]. Soohyun *et al.* revealed that perovskite solar cell is severely degraded under forward bias (>1 V), even with dark condition[17]. Deng *et al.* monitored the electric field induced both irreversible (>0.4 V μm^{-1}) and reversible (<0.4 V μm^{-1}) PL response in $CH_3NH_3PbI_3$ in air with a relative humidity of 40%[18]. Yuan *et al.* presented a reversible conversion between $MAPbI_3$ and lead iodide phases under a small electric field (3 V μm^{-1}) in air[19].

[1]Guangdong University Key Lab for Advanced Quantum Dot Displays and Lighting, Shenzhen Key Laboratory for Advanced Quantum Dot Displays and Lighting, Department of Electrical & Electronic Engineering, Southern University of Science and Technology, Shenzhen, 518055, China. [2]Department of Chemistry, Tsinghua University, Beijing, 100084, China. [3]Shenzhen Planck Innovation Technologies Pte Ltd, Ganli 6th Road, Longgang, Shenzhen, 518112, China. Bing Xu and Weigao Wang contributed equally. Correspondence and requests for materials should be addressed to X.W.S. (email: sunxw@sustc.edu.cn)

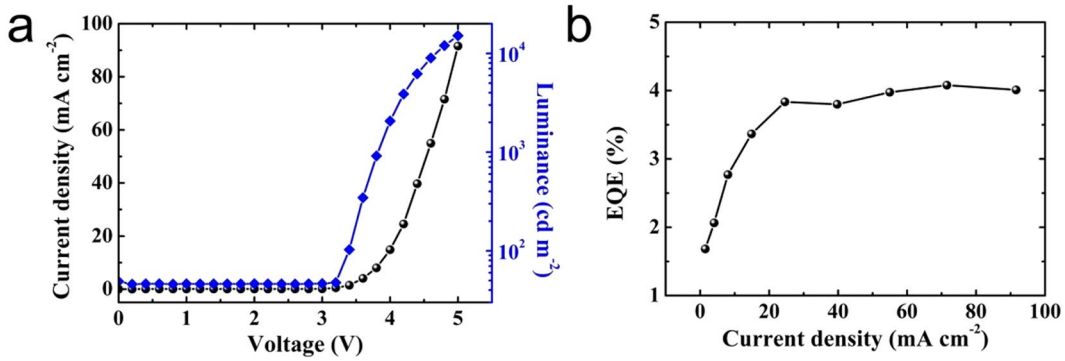

Figure 1. (**a**) Current density and luminance versus voltage and (**b**) EQE versus current density of PeLED measured after fabrication.

Recently, Zhao *et al.* observed an interesting phenomenon that for pure $MAPbI_3$ PeLEDs under the influence of subsequent electrical scans, the EQE was improved from an initial 5.9% to 7.4%[22]. This observation is different from what are often observed, where electrical bias/scan generally degrade the device. It was suspected that ion migration is the root cause of this improvement in Zhao's experiment. There is a pressing need for understanding the mechanisms behind. In this work, electrical bias effect on PeLED has been systematically studied. It is shown that electrical bias can improve or degrade the device performance depending on the magnitude of the bias. By investigating absorbance, SEM surface image and energy dispersive X-ray spectroscopy (EDX) data including point and mapping analysis of perovskite layer before and after electrical bias, the improvement and degradation effect under different electrical bias can be understood.

Experimental Section

Synthesis of $MAPbBr_3$ Nanocrystals. First MABr was synthesized by mixing the same mole ratio of methylamine (30% in methanol) and hydrobromic acid (48% in water) at 0 °C for 2 h with stirring. The precipitate was collected by evaporation of solvent at 60 °C for 1 h and purified the products by dissolving in ethanol, recrystallizing from diethl ether five times and finally dried in vacuum for 24 h.

For $MAPbBr_3$ synthesis, a 200 μL solution containing 0.1 mmol $PbBr_2$, 0.15 mmol MABr, 20 μL oleylamine and 500 μL oleic acid in dimethylformamide were added into 10 ml toluene at room temperature to produce the colloidal solution. Acetonitrile was added as a demulsifier in the demulsion process. The green product was collected after centrifugation at 5500 rpm for 4 min, then the precipitates were dissolved into 1 ml n-hexane, a bright green supernatant was obtained after another centrifugation at 5000 rpm for 4 min.

Fabrication of PeLEDs. $MAPbBr_3$ perovskite LEDs were fabricated using ITO patterned glass substrates with a sheet resistance of 15 Ω sq^{-1}. ITO substrates were sequentially cleaned using soapy water, deionized water, isopropylalcohol, and acetone in ultrasonicator for 20 min each, and then treated with O_2 plasma for 30 min prior to film deposition. PEDOT:PSS was spin-coated onto ITO substrates at 3000 rpm followed by thermal annealing at 130 °C for 20 min in air. Then these ITO substrates were transferred into N_2 glove box for further use. TFB in chlorobenzene was spin-coating on top of PEDOT:PSS at 4000 rpm, baked at 120 °C for 20 min. Perovskite were deposited at 2000 rpm without any annealing. Finally, TPBi, LiF and Al were deposited using thermal evaporation at rate of 1.0, 0.1 and 1.0 nm s^{-1}, respectively, under a high vacuum ($<1.5 \times 10^{-6}$ Torr). The device area was 2×2 mm^2.

Characterization

The EL spectra of the PeLED were measured with a fiber optic spectrometer (Ocean Optics USB2000). Device performance was achieved consisting with a calibrated PIN-25D silicon photodiode, a dual-channel Keithley 2614B source measure unit. Light emitted from PeLEDs was absorbed by the photodiode, which had a known responsivity and was measured as photodiode current, which were monitored by Keithley source. Then these two quantities were used to calculate the EQE. Surface image and element analysis were measured by using an FE-SEM (Merlin, Carl Zeiss). The XPS measurements were performed by ESCALAB 250Xi (Thermo Fisher).

Parameters for device measurement. Voltage range: 0 V to 5 V.

Step: 0.2 V.

Pulse time (each point): 100 ms.

Electrical bias was conducted by Keithley 2400 with constant voltage (0 V, 3 V, 4 V, 5 V, 6 V) in 60 s. The device performance was measured every 10 s during the electrical bias.

Perovskite nanocrystal is synthesized based on the protocol reported in the literature[23]. And the PeLEDs were fabricated with a device structure of ITO/PEDOT:PSS/TFB/$MAPbBr_3$ perovskite/TPBi/LiF/Al shown in Fig. S1a, along with a schematic energy diagram of the device in Fig. S1b, where PEDOT:PSS and TFB are serving as a hole injection layer and hole transporting layer respectively, TPBi as electron transporting layer. The current density *vs* voltage curve is shown in Fig. 1a, which is clearly a rectifying curve of a diode. The corresponding luminance and external quantum efficiency curve is shown in Fig. 1a,b, with a maximum luminance of 15000 cd m^{-2} and a EQE

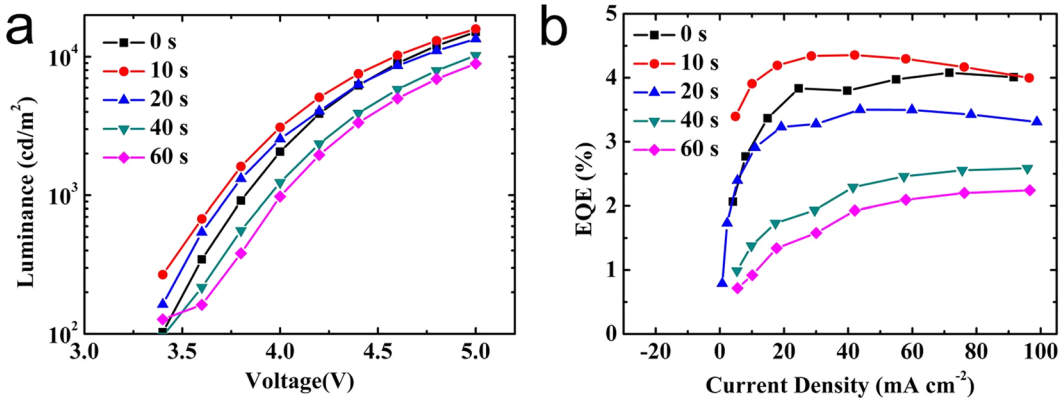

Figure 2. (**a**) Luminance versus voltage and (**b**) EQE versus current density of PeLED with subsequent scans.

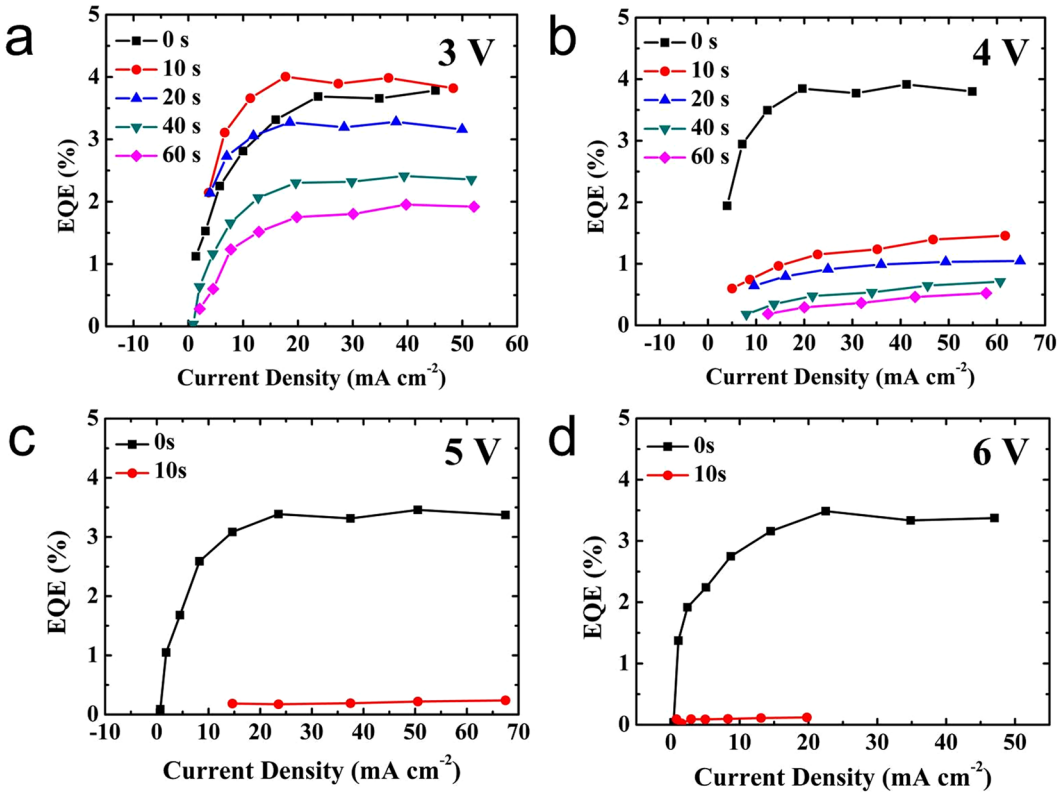

Figure 3. EQE versus current density of PeLED under different electrical bias (**a**) 3 V, (**b**) 4 V, (**c**) 5 V, (**d**) 6 V.

of 4% at 91.6 mA cm^{-2}, revealing a relatively good performance. The roll-off started at 8 V, which is no significant break down during our measurement (Fig. S2, Supporting Information).

Interestingly, we find that the luminance and EQE first increase and then decrease after several electrical scans (Fig. 2a,b). As shown in Fig. 2b, EQE increased at the second measurement, then decreased after the third measurement. But there is little change in J-V curves, as shown in Fig. S3, which indicates low emitting efficiency of PeLED. The enhancement under low current density is due to the motion of excess ions[22], like excess MA or bromide in perovskite nanocrystals fill vacancies and reduce the defects, but under high current density, the degradation of perovskite film leading to more defects, which in turn decrease device performance. The same phenomenon also happens in luminance (Fig. 2a).

In order to understand the reason behind this decrease in performance, we have applied different electrical biases to the PeLEDs (Fig. 3). Figure 3a shows the variation curve of EQE under 3 V bias for one minute. The EQE of PeLED under 3 V bias has the same trend as device without any bias. The EQE can be improved almost 20% at 15 mA cm^{-2} after 3 V 10 seconds bias, but decreases with continues bias. After applying the bias for one minute, the EQE decreased by 51% at the current of 50 mA cm^{-2}. The variation curves of EQE under 4 V, 5 V and 6 V

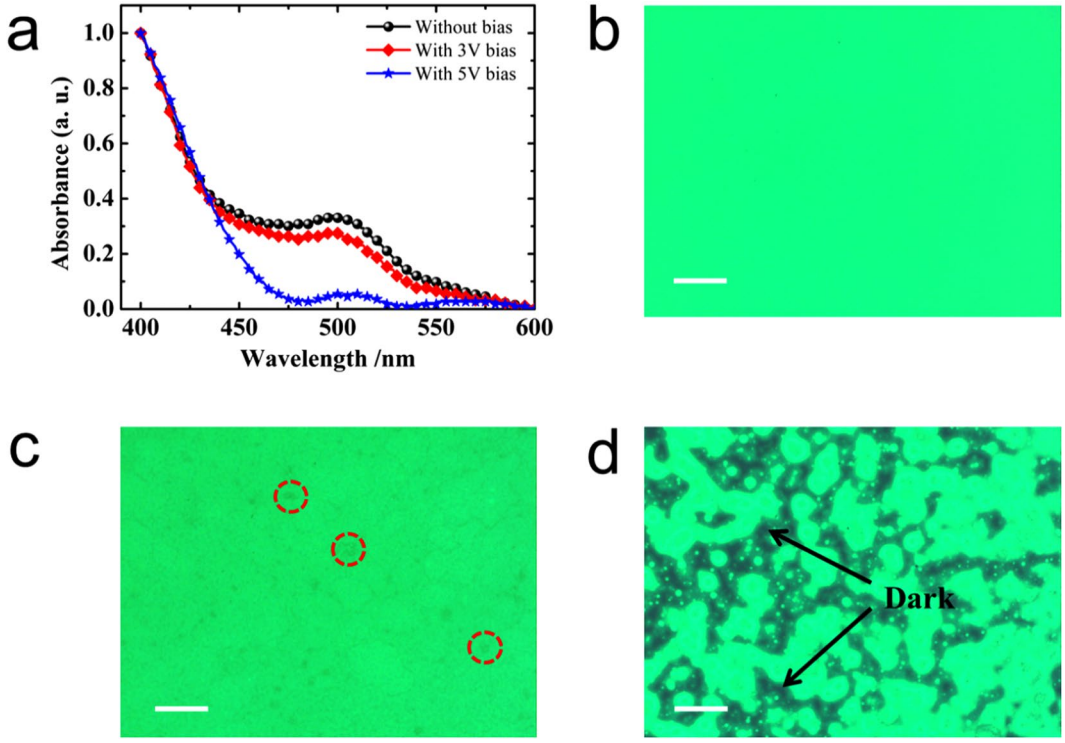

Figure 4. (**a**) Absorbance of perovskite film under different electrical bias and images of perovskite film under fluorescence microscope, (**b**) 0 V, (**c**) 3 V, (**d**) 5 V. (The structure of the samples were ITO/PEDOT:PSS/TFB/perovskite, LiF/Al was removed by tape. The scale bar is 100 μm).

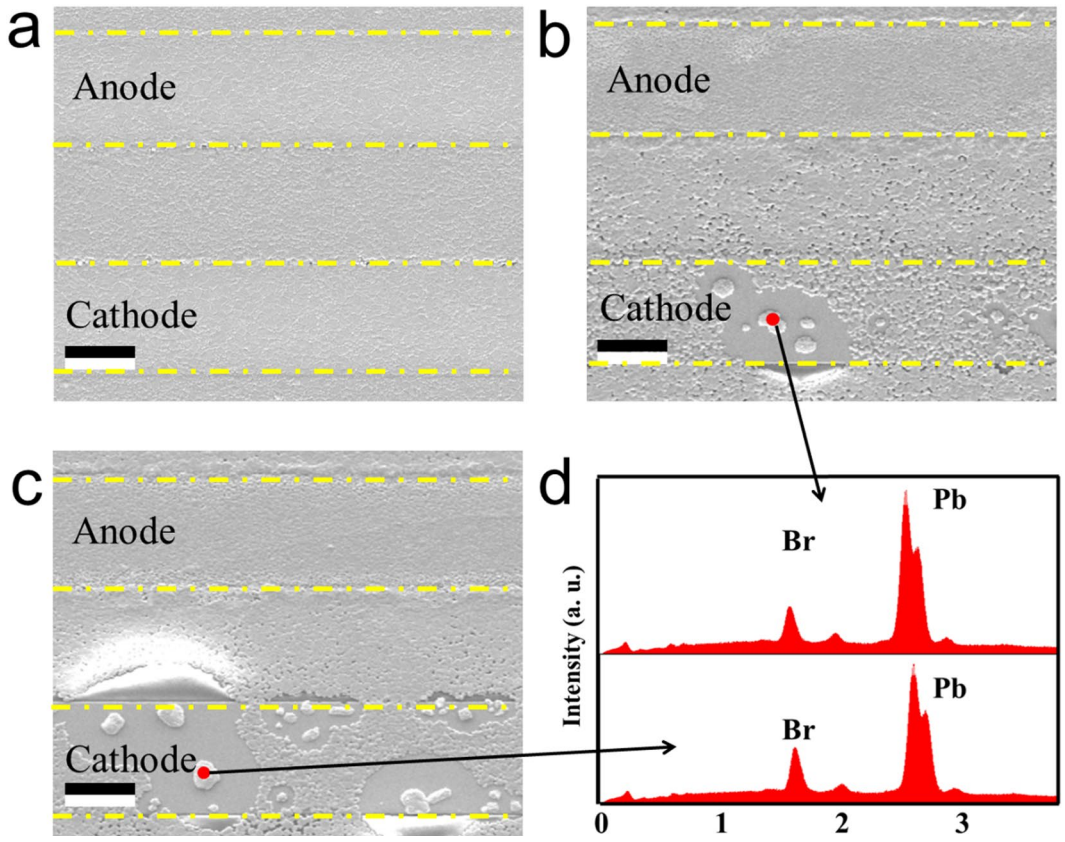

Figure 5. SEM images of perovskite film under different electrical bias in 60 s, (**a**) without electrical bias, (**b**) 3 V, (**c**) 5 V and (**d**) EDX point analysis. (The scale bar is 10 um).

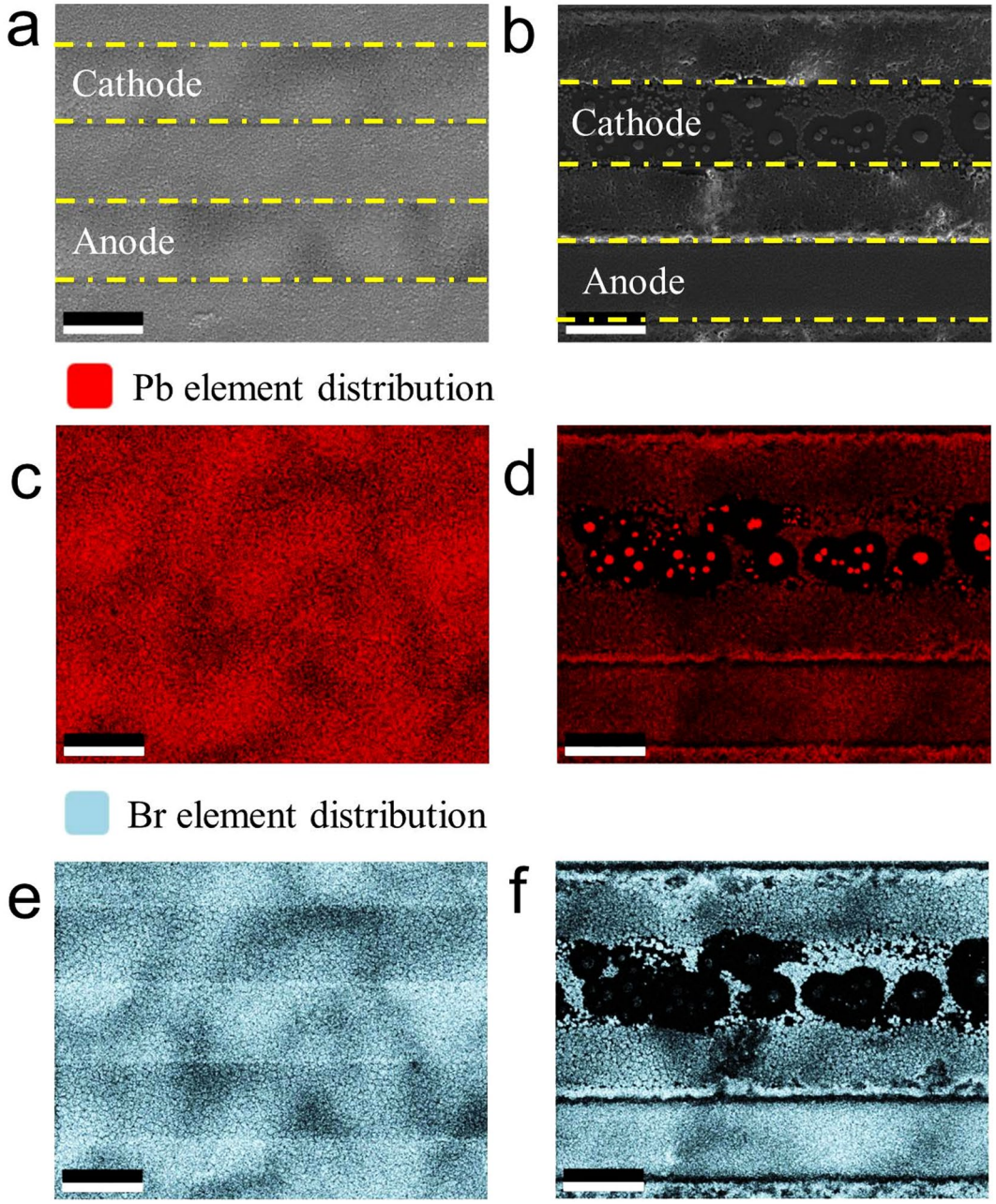

Figure 6. EDX elements mapping profile of Pb, Br after 0 V and 5 V bias. (**a**) and (**b**) are the corresponding image, (**b**,**c**,**e**,**f**) are Pb and Br distribution, respectively. (The scale bar is 20 um).

biases are different from that of 3 V bias, which shows only decay with continue electrical bias. Under 4 V continues bias (Fig. 3b), the EQE are dramatically decreased from 3.8% to 1.4% within 10 s bias stress, then decreased to 0.5% after another 50 s. The PeLED devices immediately failed under 5 V and 6 V bias stress for 10 s.

To identify the degradation products left behind after the electrical bias, we further characterize the perovskite film by measuring absorption and fluorescence microscope. In Fig. 4a, we plot the absorption of perovskite film after different electrical bias. As electrical bias increases, we observed a reduction in absorption which means the degradation of perovskite film. The fluorescence microscope images indicate that the emission of perovskite film under UV light is relative uniform without electrical bias. After electrical bias, perovskite films start to degrade which shows that there is no emission for some areas sparsely distributed across the area examination. To further confirm the degradation of perovskite film, X-ray diffraction was performed, which observed the decrease of peaks intensity for perovskite crystals (Fig. S4a). And after the electrical bias, the diffraction peak of $PbBr_2$ appears (Fig. S4b), which means $PbBr_2$ is one of decomposed products.

To further investigate the degradation mechanisms of perovskite film under electrical bias, we analyzed EDX elements distribution under different electrical bias. Figure 5 displays the morphology of perovskite film driven in one minute at three different voltages (0, 3, and 5 V). As seen in Fig. 5a, the perovskite film has smooth

morphology. Significant islands start to appear after reaching 3 V bias in one minute, and the number of these islands grows with the increase of the electrical bias accordingly. In order to find out the elemental composition of the island, we conducted the EDX point analysis, shown in Fig. 5d, which contains Pb and Br only. But C, N, Pb and Br can be detected in perovskite film before electrical bias, shown in Fig. S5. And XPS results (Fig. S6) show that there is no Pb metal peak after electrical bias. So combining with the XRD, XPS and EDX results, the possible mechanism of degradation is shown as follows[19,24]:

$$CH_3NH_3PbBr_3 \rightarrow CH_3NH_3^+ + PbBr_2 + Br^-$$
$$2Br^- \rightarrow Br_2 \uparrow + 2e^-$$

This degradation will lead to breakdown of the perovskite film, which is responsible for the decay in device performance. In order to further understand Pb and Br elements distribution, EDX mapping was conducted, as shown in Fig. 6. Before any electrical bias is applied, Pb and Br are evenly distributed across the whole perovskite film. When 5 V electrical bias is applied, leading to unevenly distribution of Pb and Br.

In conclusion, using perovskite light emitting diodes with EQE as high as 4%, we studied the degradation in PeLEDs under different electrical bias. To observe degradation induced by electrical bias, biasing tests were conducted under different voltage. Under low electrical bias, the efficiency can be improved, owing to the excess ions (like Br^-) filling vacancies. On the other hand, under long time operation or high electrical bias, the performance will immediately decay, mainly due to degradation of the perovskite film. Additionally, the degradation rate of perovskite depends on the magnitude of the forward electric bias. This work highlights the necessity of further research to improve the stability of PeLEDs.

References

1. Stranks, S. D. *et al.* Electron-Hole Diffusion Lengths Exceeding 1 Micrometer in an Organometal Trihalide Perovskite Absorber. *Science* **342**, 341–344 (2013).
2. Wehrenfennig, C., Eperon, G. E., Jonston, M. B., Snaith, H. J. & Hertz, L. M. High Charge Carrier Mobilities and Lifetimes in Organolead Trihalide Perovskites. *Adv. Mater.* **26**, 1584–1589 (2014).
3. Green, M. A., Ho-Baillie, A. & Snaith, H. J. The emergence of perovskite solar cells. *Nat. Photonics* **8**, 506–514 (2014).
4. Green, M. A., Jiang, Y., Soufiani, A. M. & Ho-Baillie, A. Optical Properties of Photovoltaic Organic-Inorganic Lead Halide Perovskites. *J. Phys. Chem. Lett.* **6**, 4774–4785 (2015).
5. Dong, Q. *et al.* Electron-hole diffusion lengths >175 μm in solution grown $CH_3NH_3PbI_3$ single crystals. *Science* **347**, 967–970 (2015).
6. National Renewable Energy Laboratory (NREL), Efficiency Chart, https://www.nrel.gov/pv/assets/images/efficiency-chart-20180716.jpg.
7. Song, J. *et al.* Quantum Dot Light-Emitting Diodes Based on Inorganic Perovskite Cesium Lead Halides. *Adv. Mater.* **27**, 7162–7167 (2015).
8. Zhang, X. *et al.* Enhancing the Brightness of Cesium Lead Halide Perovskite Nanocrystal Based Green Light-Emitting Devices through the Interface Engineering with Perfluorinated Ionomer. *Nano Lett.* **16**, 1415–1420 (2016).
9. Li, X. *et al.* $CsPbX_3$ Quantum Dots for Lighting and Displays: Room-Temperature Synthesis, Photoluminescence Superiorities, Underlying Origins and White Light-Emitting Diodes. *Adv. Funct. Mater.* **26**, 2435–2445 (2016).
10. Zhang, F. *et al.* Brightly Luminescent and Color-Tunable Colloidal $CH_3NH_3PbX_3$ (X = Br, I, Cl) Quantum Dots: Potential Alternatives for Display Technology. *ACS Nano* **9**, 4533–4542 (2015).
11. Tan, Z. K., Moghaddam, R. S., Lai, M. L., Snaith, H. J. & Friend, R. H. Bright light-emitting diodes based on organometal halide perovskite. *Nat. Nanotechnol.* **9**, 687–692 (2014).
12. Cho, H. *et al.* Overcoming the electroluminescence efficiency limitations of perovskite light-emitting diodes. *Science* **350**, 1222–1225 (2015).
13. Wang, J. *et al.* Interfacial Control Toward Efficient and Low-Voltage Perovskite Light-Emitting Diodes. *Adv. Mater.* **27**, 2311–2316 (2015).
14. Yuan, M. *et al.* Perovskite energy funnels for efficient light-emitting diodes. *Nat. Nanotechnol.* **11**, 872–877 (2016).
15. Xiao, Z. *et al.* Efficient perovskite light-emitting diodes featuring nanometre-sized crystallites. *Nat. Photonics* **11**, 108–115 (2017).
16. Leijten, T. *et al.* Stability of Metal Halide Perovskite Solar Cells. *Adv. Energy Mater.* **5**, 1500963 (2015).
17. Bae, S. *et al.* Electric-field-induced degradation of methylammonium lead iodide perovskite solar cells. *J. Phys. Chem. Lett.* **7**, 3091–3096 (2016).
18. Deng, X. *et al.* Electric field induced reversible and irreversible photoluminescence responses in methylammonium lead iodide perovskite. *J. Mater. Chem. C* **4**, 9060–9068 (2016).
19. Yuan, Y., Wang, Q., Shao, Y., Lu, H. & Huang, J. Electric-Field-Driven Reversible Conversion Between Methylammonium Lead Triiodide Perovskites and Lead Iodide at Elevated Temperatures. *Adv, Energy Mater.* **6**, 1501803 (2016).
20. Li, D., Wu, H., Cheng, H. C., Wang, G., Huang, Y. & Duan, X. Electronic and ionic transport dynamics in organolead halide perovskites. *ACS Nano* **10**, 6933–6941 (2016).
21. DeQuilettes, D. W. *et al.* Photo-induced halide redistribution in organic-inorganic perovskite films. *Nature Communication* **7**, 11683 (2016).
22. Zhao, L. *et al.* Electrical Stress Influences the Efficiency of $CH_3NH_3PbI_3$ Perovskite Light Emitting Devices. *Adv. Mater.* **29**, 1605317 (2017).
23. Zhang, X. *et al.* Hybrid Perovskite Light-Emitting Diodes Based on Perovskite Nanocrystals with Organic-Inorganic Mixed Cations. *Adv. Mater.* **29**, 1606405 (2017).
24. Berhe, T. A. *et al.* Organometal halide perovskite solar cells: degradation and stability. *Energy Environ. Sci.* **9**, 323–356 (2016).

Acknowledgements

The National Key Research and Development Program of China administrated by the Ministry of Science and Technology of China (No. 2016YFB0401702), National Natural Science Foundation of China (No. 61674074 and 61405089), Shenzhen Peacock Team Project (No. KQTD2016030111203005), Shenzhen Key Laboratory for Advanced quantum dot Displays and Lighting (No. ZDSYS201707281632549), Shenzhen Innovation Project (No. JCYJ20160301113356947), Guangdong University Key Laboratory for Advanced Quantum Dot Displays and Lighting (No. 2017KSYS007), Distinguished Young Scholar of National Natural Science Foundation of Guangdong (No. 2017B030306010), and also thanks the start-up fund from Southern University of Science and Technology.

Author Contributions

X.W. Sun, L.D. Wang and K. Wang conceived the study and designed the experiments. B. Xu performed the synthesis of perovskite nanocrystals, measured the performance of PeLED and wrote the paper. W.G. Wang fabricated PeLED devices. H.C. Liu helped with SEM measurements. Y.N. Zhang and G.D. Mei helped with absorption measurements. S.M. Chen and X.L. Zhang advised on improvement of device fabrication. All authors reviewed the manuscript.

Additional Information

Supplementary information accompanies this paper at https://doi.org/10.1038/s41598-018-34034-1.

Competing Interests: The authors declare no competing interests.

Publisher's note: Springer Nature remains neutral with regard to jurisdictional claims in published maps and institutional affiliations.